Boundary element analysis for primary and secondary creep problems

E. Pineda León
Escuela Superior de Ingeniería y Arquitectura, Instituto Politécnico Nacional,
U.P. Adolfo López Mateos, Zacatenco, 07738, México D.F., México,
e-mail: epinedal@ipn.mx.

M.H. Aliabadi
Department of Aeronautical Engineering, Imperial College London,
South Kensington campus, London SW7 2AZ.

M. Ortiz-Dominguez
Instituto Politécnico Nacional. SEPI-ESIME,
U.P. Adolfo López Mateos, Zacatenco, 07738, México D.F., México.

Recibido el 11 de abril de 2007; aceptado el 7 de julio de 2008

This paper presents the application of the Boundary Element Method to primary and secondary creep problems in a two-dimensional analysis. The domain, where the creep phenomena takes place, is discretized into quadratic, quadrilateral, continuous internal cells. The creep analysis is basically applied to metals, that are capable of modeling secondary and primary creep behaviour. This is confined to standard power law creep equations. Constant applied loads are used to demonstrate time effects. Numerical results are compared with solutions obtained from the Finite Element Method (FEM) and references.

Keywords: Creep; boundary element method; finite element method

Este artículo presenta la aplicación del Método de Elementos de Frontera a problemas del creep primarios y secundarios para un análisis en dos dimensiones. El dominio, donde el fenómeno del creep se genera, es dicretizado con celdas internas cuadriláteras cuadráticas continuas. El análisis del creep es básicamente aplicado a metales, que son capaces de modelar el comportamiento primario y secundario del creep. Dicho comportamiento está limitado a ecuaciones de la ley de potencia del creep. Se aplican cargas constantes para demostrar los efectos del tiempo. Los resultados numéricos son comparados con soluciones obtenidas del Método de Elementos Finitos y referencias.

Descriptores: Creep; elementos de frontera; elementos finitos.

PACS: 62.20.Hg; 43.20.Rz; 47.11.Fg

1. Introduction

Most of the materials used in engineering have sophisticated material properties which may depend on stress, time and temperature. In order to model the complex behaviour of such materials, stress analysis techniques are developed. These techniques are necessary to solve the elastic problem but also go further to model the non-elastic phenomenon such as plasticity and creep.

For many years the FEM has been used as the main tool to solve problems in engineering [2]. The domain of the body is divided into several small subdomains, of a fairly simple shape, called finite elements. Any continuous parameter such as pressure or displacement can be approximated to the actual behaviour of the solution with trial functions, usually polynomials. These functions are uniquely defined in terms of the approximated values of the solution at some nodal points, inside or on the boundary of each element.

A weighted residual technique is the most popular tool to assess this approximation, leading to a symmetric system of equations which involves the unknown values of the approximated solution at nodal points. Without doubt this method is computationally efficient and for many years has reached such popularity that a very wide range of linear and nonlinear engineering problems have been solved with this powerful numerical method [3].

The Boundary Element Method (BEM) is a less mature technique but has reached a level of development in certain fields that has made it an essential tool for design engineers. The BEM has also many applications but not as many as FEM. Nevertheless this method is an effective alternative to FEM in many important areas of engineering analysis. The BEM is a relatively new technique for engineering analysis; the fundamental can be traced back to mathematical formulations by Fredholm [4] and Mikhilin [5] in potential theory and Kupradze [6] in elasticity. In the context of the BEM, also called Boundary Integral Equation (BIE) [7], the formulations are due to Jaswon [8], Hess and Smith [9], Massonet [10], Rizzo [11] and Cruse [12]. But perhaps the most significant early contribution to BEM as an effective numerical technique is due to the work of Lachat [13] and Lachat and Watson [14]. They developed an isoparametric formulation similar to the FEM and proved that the BEM can be used as an efficient tool for solving problems with sophisticated configurations.

The reduction of the dimensionality of the problem is one of the most important attractive features of this technique; in the two-dimensional case, only the boundary of the domain needs to be discretized and for three-dimensional problems, the surface is discretized into a number of boundary elements over which polynomial functions, of the type used in finite elements, are introduced to interpolate the values of the approximated solution between the nodal points. Following discretization of the boundary and the evaluation of the relevant integrals, a matrix system of equations is obtained, which is fully populated and non-symmetric, and is of a much smaller size than the FEM.

Some of the main characteristics of BEM are:

i) a reduced set of equations,

ii) simple data preparation,

iii) semi-infinite or infinite boundaries need not be accurately modeled,

iv) accurate selective calculation of internal stresses and

v) displacements and high resolution for stress concentration problems.

These features plainly justify the increasing popularity achieved in recent years.

This paper is dedicated to the creep analysis by applying the Boundary Element Method (BEM) in order to find a more efficient and accurate analysis technique.

2. Methodology

2.1. Introduction to Creep

The phenomenon of creep can be illustrated by considering a specimen which is loaded at room temperature. If the load is applied for a long period of time, under constant temperature, the specimen gradually deforms in time. This behaviour may eventually fail after intervals ranging from minutes to many years depending on the temperature and the applied load. At low temperatures changes due to creep are usually very small and failure rarely occurs. At high temperatures, creep deformation can cause considerable changes in dimensions and failure generally occurs after a certain time, t_f. The time to fracture decreases if both the temperature and the applied stress are increased. Because of this, it is important to define the high temperatures at which creep and creep fracture generally become important. In the case of pure metals, high temperatures can be defined at about 0.4 Tm, where Tm is the absolute melting point.

2.2. Power Law Creep Model

The expression commonly used to describe accurately the way the secondary creep rate varies with the stress by applying the same temperature is:

$$\dot{\varepsilon}^c = \sigma^n \tag{1}$$

where n is a material constant, $\dot{\varepsilon}^c$ is the creep strain rate since the (.) denotes the derivative with respect to time, t. In expression (1), is clear that the stress-creep strain rate relationship is non-linear. This equation provides the basis for "power law creep" relationships, which have been widely used to represent the behaviour of the high-temperature creep.

From the mathematical model for stress dependence and time dependence, the strain for secondary creep can be modeled as:

$$\dot{\varepsilon}^c = B\sigma^n t$$

where B is a material constant that depends on the temperature.

The Norton-Bailey equations are combined to obtain the expression for representing primary and secondary creep at a constant temperature:

$$\dot{\varepsilon}^c = B\sigma^n t^m \tag{2}$$

where m is a material property that indicates the creep stage.

2.3. Creep behaviour Under Variable Uniaxial Stress

The analysis of the constant uniaxial stress creep model has served to define the basic dependence of the deformation on time, temperature and stress. For varying stress, the theory of creep is more complicated and two approaches have to be considered: the time hardening approach, and the strain hardening approach. By differentiating the Norton-Bailey equation [see Eq. (2)], with respect to time, the creep strain rate can be written as follows:

$$\dot{\varepsilon}^c = mB\sigma^n t^{(m-1)} \tag{3}$$

This equation is called the *time hardening approach* and the creep strain rate depends on the current stress and time. By substituting $m < 1$ in the above equation we obtain the primary creep stage. The substitution of $m = 1$ into (3) describes the secondary creep stage, which becomes:

$$\dot{\varepsilon}^c = B\sigma^n, \tag{4}$$

where the dot above the strain indicates the rate of change with time. According to the above equation, the creep strain rate at this stage depends on the current stress only.

2.4. Multiaxial States of Stress

In practice, it is found that the multiaxial characteristics of creep are very similar to non-linear formulations, and are commonly based on the Prandtl-Reuss flow rule and the von Mises effective stress criterion.

So, the multiaxial case of the time hardening approach is obtained as follows

$$\dot{\varepsilon}^c = \frac{3}{2} mB(\sigma_{eq})^{(n-1)} S_{ij} t^{(m-1)}$$

The above multiaxial formulation is based on the uniaxial creep law, and therefore it is not suitable for stress reversal situations.

2.5. Non-Linear formulation for BEM

The equilibrium conditions that must be satisfied over the domain can be represented in terms of rates as follows:

$$\dot{\sigma}_{ij,i} + \dot{b}_j = 0, \tag{5}$$

and on the boundary:

$$\dot{t}_i - \dot{\sigma}_{ij} n_j = 0, \tag{6}$$

where $\dot{b}_j$are the body forces and n_j are the components of the outward normal to the boundary.

The relationship for the total stress and strain, elastic and inelastic, in term of rate quantities can be written as follows:

$$\dot{\sigma}_{ij} = \dot{\sigma}^e_{ij} + \dot{\sigma}^a_{ij},$$
$$\dot{\varepsilon}_{ij} = \dot{\varepsilon}^e_{ij} + \dot{\varepsilon}^a_{ij}.$$

where$\dot{\sigma}^e_{ij}$, $\dot{\sigma}^a_{ij}$are the elastic and inelastic stress tensor, respectively. Here $\dot{\varepsilon}^e_{ij}$ and $\dot{\varepsilon}^a_{ij}$ are the elastic and inelastic strain, respectively.

The inelastic stress tensor (see Ref. 1), can be defined by the following equation:

$$\dot{\sigma}^a_{ij} = 2\mu\dot{\varepsilon}^a_{ij} + \frac{2\mu\nu}{1-2\nu}\dot{\varepsilon}^a_{kk}\delta_{ij},$$

where $\dot{\varepsilon}^a_{kk}$ is the inelastic strain rate of the main diagonal and δ_{ij} is the Kronecker delta whose properties are

$$\delta_{ij} = \begin{cases} 0, \text{ if i = j} \\ 1, \text{ if i} \neq \text{j} \end{cases}.$$

The inelastic part of the stress and strain rate $\left(\dot{\sigma}^a_{ij}, \dot{\varepsilon}^a_{ij}\right)$ can include any kind of inelastic strain such as plastic, creep or others (see Ref. 20). The superscript ^{a} is used, instead of ^{c}, in order to indicate that the formulation is general, even though the work carried out in this paper deals exclusively with inelastic strains caused by creep.

In terms of displacements, Navier's equations for non-linear analysis can be developed as in elasticity, so the governing differential equations of the problem are obtained, but now the rate form of the equations instead. The substitution of the relationship between the stress and the strain rates in terms of displacements into the equilibrium equation gives

$$\left(2\mu\dot{\varepsilon}_{ij} + \frac{2\mu\nu}{1-2\nu}\dot{\varepsilon}_{kk}\delta_{ij} - \dot{\sigma}^a_{ij}\right)_{,i} + \dot{b}_j = 0; \tag{7}$$

by applying the Kronecker delta and substituting $\dot{\sigma}^a_{ij}$ in Eq. (7) it is possible to obtain

$$\mu\dot{u}_{j,jl} + \mu\left(\frac{1}{1-2\nu}\right)\dot{u}_{j,jl} - 2\mu\dot{\varepsilon}^a_{jj,l} - \frac{2\mu\nu}{1-2\nu}\dot{e}_{,l} + \dot{b}_j = 0, \tag{8}$$

where $\dot{e} = \dot{\varepsilon}^a_{kk}$ *i.e.* inelastic strain rate. Equation (8) is for internal points, but boundary conditions must be also satisfied. The boundary conditions in terms of rates are; for displacements $\dot{u}_i = \ddot{u}_i$ and for tractions $\dot{t}_i = \ddot{t}_i$ and the equation representing the traction boundary conditions (see Ref. 1) is

$$\dot{t}_i + 2\mu\left(\dot{\varepsilon}^a_{ij} + \frac{\nu}{1-2\nu}\dot{e}\right)n_j = \frac{2\mu\nu}{1-2\nu}\dot{u}_{l,l}n_i + \mu\left(\dot{u}_{i,j} + \dot{u}_{j,i}\right)n_j. \tag{9}$$

Equations (8) and (9) are for three-dimensional problems. In order to work with two-dimensional problems for the plane stress state, it is necessary to remove the strain in the z-direction, so $\dot{\varepsilon}^a_{33} = 0$.

So far the non-linear problem has been analyzed, which means that it is not possible to solve the resulting governing equations directly, as in elasticity. It is possible to solve the non-linear problem by using a method that involves essentially the solution of an elastic problem in each iteration; this method is called the *successive elastic solution* and it is used in this work.

The displacement boundary integral equation for inelasticity (see Ref. 1) can be summarized as follows:

$$\int_\Omega \dot{\sigma}'_{ij,j}\dot{u}_i d\Omega + \int_\Gamma \dot{\sigma}'_{ij}n_j\dot{u}_i d\Gamma - \int_\Omega \dot{\sigma}'_{ij}\dot{\varepsilon}^a_{ij}d\Omega = \int_\Omega \dot{\sigma}_{ij,j}\dot{u}'_i d\Omega + \int_\Gamma \dot{\sigma}_{ij}n_j\dot{u}'_i d\Gamma, \tag{10}$$

where Ω' is a domain containing Ω, and Γ is the boundary contained in the domain Ω.

The equilibrium equations and traction definition $(\dot{t}_i = \dot{\sigma}_{ij}n_j)$ can be substituted into Eq. (10) to obtain

$$\int_\Omega \dot{b}'_i\dot{u}_i d\Omega + \int_\Gamma \dot{t}'_i\dot{u}_i d\Gamma - \int_\Omega \dot{\sigma}'_{ij}\dot{\varepsilon}^a_{ij}d\Omega = \int_\Omega \dot{b}_i\dot{u}'_i d\Omega + \int_\Gamma \dot{t}_i\dot{u}'_i d\Gamma, \tag{11}$$

where $\dot{u}_i, \dot{t}_i, \dot{\sigma}_{ij}$ and $\dot{\varepsilon}_{ij}$ are the displacement, traction, stress and strain rates, respectively, that belong to the domain Ω. Here $\dot{u}'_i, \dot{t}'_i, \dot{\sigma}'_{ij}$ and $\dot{\varepsilon}'_{ij}$ are the fields corresponding to the domain Ω'. This leads to the following boundary integral representation of the boundary displacements when the initial strain approach is used for the solution of inelastic problems:

$$c_{ij}\dot{u}_j + \oint_\Gamma \dot{t}'_{ij}\dot{u}_j d\Gamma = \int_\Gamma \dot{u}'_j\dot{t}_{ij}d\Gamma + \int_\Omega \dot{\sigma}'_{ijk}\dot{\varepsilon}^a_{jk}d\Omega. \tag{12}$$

In a similar way, the boundary integral equation of the internal stresses is expressed by

$$\dot{\sigma}_{ij} = \int_\Gamma D_{ijk}\dot{t}_j d\Gamma - \int_\Gamma S_{ijk}\dot{u}_j d\Gamma + \oint_\Omega \Sigma_{ijk}\dot{\varepsilon}^a_{jk}d\Omega + f_{ij}\dot{\varepsilon}^a_{jk} \tag{13}$$

where $\oint$ is a Cauchy integral, D_{ijk} and S_{ijk} are terms containing the derivative of the displacements and tractions, f_{ij} is the free term and Σ_{ij} is the fundamental solution for the domain.

The solution to Navier's differential equation through the use of the Galerking vector is called the fundamental solution for a unit force point applied to the body at point d.

The displacement and tractions fundamental solutions, see Ref. 1 for the displacement boundary equation in the two-dimensional planes are

$$\dot{u}'_i = \frac{1}{8\pi\mu\,(1-\nu)}\left[(3-4\nu)\ln\left(\frac{1}{r}\right)\delta_{ij} + r_{,i}r,j\right] \quad (14)$$

$$\dot{t}'_{ij} = \frac{-1}{4\pi\,(1-\nu)\,r}\{[(1-2\nu)\,\delta_{ij} + 2r_{,i}r_{,j}]\,\frac{\partial r}{\partial n} - (1-2\nu)\,(r_{,i}n_j - r_{,j}n_i)\} \quad (15)$$

$$\sigma'_{ijk} = \frac{-1}{4\pi\,(1-\bar{\nu})\,r}\{((1-2\nu)\,(r_{,j}\delta_{ki} + r_{,i}\delta_{jk} - r_{,k}\delta_{ij})) + 2r_{,i}r_{,j}r_{,k}\} \quad (16)$$

2.6. Boundary Integral Formulation on Creep

In creep analysis, as in plasticity, the initial strain approach will be applied and the integral equation to calculate the displacement on the boundary is basically the same; the only difference is that the plastic strain is replaced with the creep strain rate. So the displacement equation (14) can be rewritten as:

$$c_{ij}(x')\dot{u}_j(x') + \int_\Gamma t'_{ij}(x',x)\dot{u}_i(x')d\Gamma = \int_\Gamma u'_{ij}(x',x)\dot{t}_j(x')d\Gamma + \int_\Omega \sigma'_{ij}\,(x',z)\,\dot{\varepsilon}^c_{ij}\,(z)\,, \quad (17)$$

where $\dot{u}_i$, $\dot{t}_i$ and $\dot{\varepsilon}^c_{ij}$ are the displacement, traction and creep strain rates, respectively. t'_{ij}, u'_{ij} and $\sigma'_{ij}$are the displacement, traction and third order fundamental solutions, respectively, which are functions of the positions of the collocation point x′ and the field point x which belong to the boundary, or the internal point z and the material properties.

2.7. Singularities

Two different kinds of integrals can be defined for both the boundary and the domain. Depending on the integrands, integrals can be classified as: Regular, in which case they can be evaluated using the standard gauss quadrature rule, or Singular, when the collocation point belongs to the element over which the integration is performed, in which case special techniques must be used.

All the singular integrals appearing in the displacement and internal stress integral equations are dealt with by using well established techniques and are treated separately based on their order of singularity.

On the boundary, near-singular integrals (when the collocation node is close to the integration element) are treated with the element subdivision technique [1]. Weakly singular integrals O(lnr) are treated using a nonlinear coordinate transformation, as reported by Telles [19]. Strongly singular integrals O(1/r) are computed indirectly by considering the generalized rigid body motion, as explained in [20].

The domain singular integrals can also be separated into weak O(1/r) and strong O($1/r^2$). Weakly singular integrals are treated by a simple technique such as polar coordinate transformation, followed by a regular procedure [1]. Strongly singular integrals require special techniques such as those described by Leitao [20].

2.8. Equivalent Stress

Since the material properties such as the hardening parameters and the yield stress are obtained from uniaxial loading tests, it is necessary to state a correlation between them and the multiaxial stress state. These can be through the equivalent quantities namely: the equivalent or effective stress. The equivalent or effective stress can be defined as

$$\sigma_{eq} = \sqrt{3J_2} = \sqrt{\frac{3}{2}S_{ij}S_{ij}} \quad (18)$$

Where J_2 is the deviatoric stress tensor and

$$S_{ij} = \sigma_{ij} - \frac{\nu}{1+\nu}\sigma_{kk}\delta_{ij}$$

(see Ref. 22).

2.9. Numerical Integration

The domain$\Omega_Y$is divided into N_c cells as follows:

$$\Omega_Y = \overset{N_c}{\underset{n=1}{U}}\,\Omega_n. \quad (19)$$

The plastic terms for the strain and stress rate tensors are given, at every cellΩ_n, by

$$\dot{\varepsilon}^a_{ij} = \sum_{L=1}^{n_c}\Psi_L\dot{\varepsilon}^{a,k}_{ij} \quad (20)$$

$$\dot{\sigma}^a_i = \sum_{L=1}^{N_c}\Psi_L\dot{\sigma}^{a,k}_{ij} \quad (21)$$

where n_c is the number of nodes in the cell, $N_c$is the number of cells and Ψ_L are the shape functions. The numerical expression for the displacement on the boundary is

$$c\dot{u} + \sum_{n=1}^{N_{el}}\left(\int_\Gamma T\phi d\Gamma\right)\dot{u}^n = \sum_{n=1}^{N_{el}}\left(\int_\Gamma U\phi d\Gamma\right)\dot{t}^n + \sum_{n=1}^{N_{el}}\left(\int_{\Omega_N}\sigma\Psi d\Omega\dot{\varepsilon}^{g,n}\right) \quad (22)$$

The terms T, U and σ in this equation, are sub-matrices containing the fundamental solution. N_{el} is the number of integration elements. Similarly to the boundary, the discretized expression for the domain stresses can be obtained by

$$\dot{\sigma}_{ij} = \sum_{n=1}^{N_{el}} \int_{\Gamma} D\dot{t} d\Gamma - \sum_{n=1}^{N_{el}} \int_{\Gamma} S\dot{u} d\Gamma + \sum_{n=1}^{N_{el}} \int_{\Omega} \Sigma \Psi d\Omega \dot{\varepsilon}^{g,n} + f_{ij}\left(\dot{\varepsilon}^{g}\right) \quad (23)$$

The quantities D, S and Σ are sub-matrices containing the derivative of the fundamental solution, and Ψ are the shape functions corresponding to the boundary elements and cells, respectively.

3. Results

3.1. Primary Creep Problems

All the results are presented for node 1. An automatic time marching scheme with the maximum and the minimum creep strain tolerances of 10^{-3} and 10^{-4} are used in all the examples. Also the geometry, mesh, material properties and creep parameters are presented in Fig. 1, except that the applied load is different in every case. Every test is performed for the total time of 1000 hours for the full load approach.

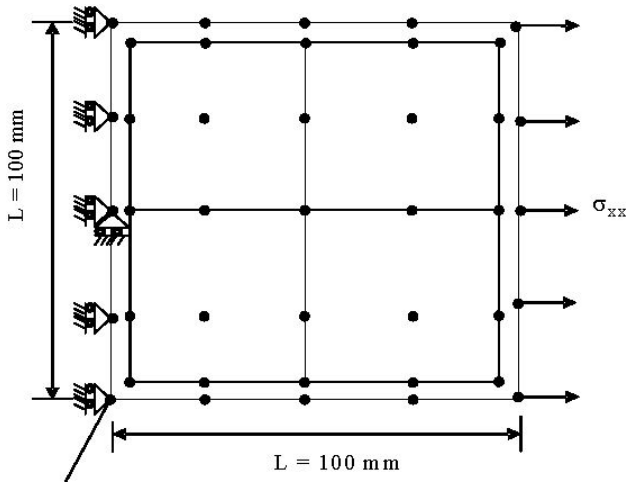

FIGURE 1. Geometry, mesh and boundary conditions for a square plate.

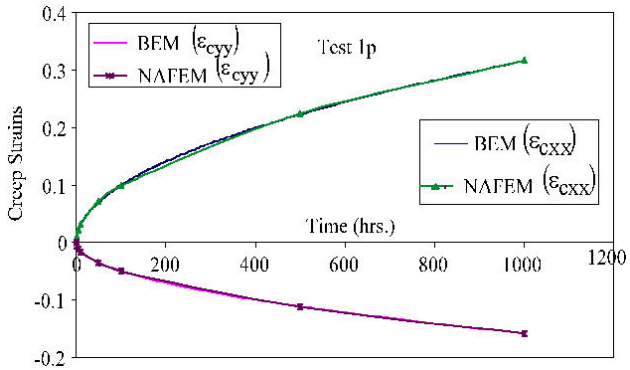

FIGURE 2. Creep strains for uniaxial load in a primary creep analysis.

3.2. Test 1p: Plane Stress (Uniaxial Load)

A square plate subjected to a tensile stress of 200 N/mm^2 in the x-direction is used in this example. The mesh consists of 8 boundary elements and 4 internal cells, as shown in Fig. 1. A uniaxial stress distribution is involved in this test.

The elastic material properties are:

Young's modulus, $E = 200 \times 10^3$N/mm^2.;

Poisson's ratio, =0.3;

Applied stress, $\sigma_{xx} = 200$ N/mm^2.

Hardening coefficient H/=0

Creep parameters	Total creep time
$B = 3.125 \times 10^{-14}$ (MPa./hr.)	$T_c = 1000$ hrs.

m=0.5 (Primary creep)

n=5

The results at the final time are presented in Fig. 2. The creep strains for both directions x and y have a parabolic behaviour, which is to be expected for primary creep analysis. The results are in very good agreement with the results presented in NAFEMS's report (see Ref. 21).

3.3. Test 2p: Plane Stress (Biaxial Load)

A square plate subjected to biaxial tensile stress is used in this example. This test is a primary creep and plane stress problem. There is an additional applied load in the y-direction, σ_{yy} = 200N/mm^2.

The results of the effective or equivalent creep strain and the creep strain in x-direction are presented in Fig. 3. These results show the parabolic behaviour of the primary creep analysis which is expected for this stage of creep. These results are in very good agreement with NAFEMS' results.

3.4. Test 3p: Plane stress (biaxial negative load)

This example is subjected to biaxial stress, similar to test 2p. This test is a primary creep and plane stress problem. The geometry, material, mesh, properties and creep parameters are the same as those used in test 2p, except that there is compression applied in the y-direction, σ_{yy} =-200N/mm^2.

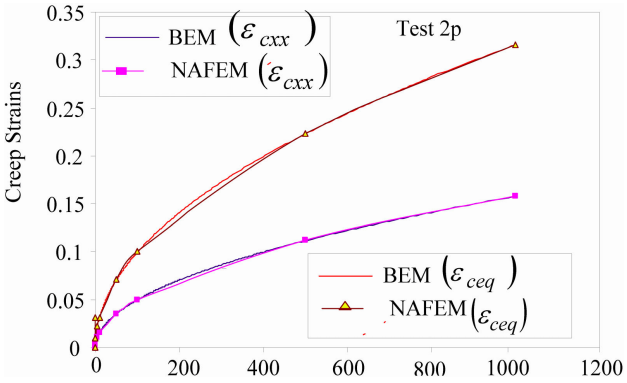

FIGURE 3. Equivalent creep strain distribution and strain in x-direction for biaxial load.

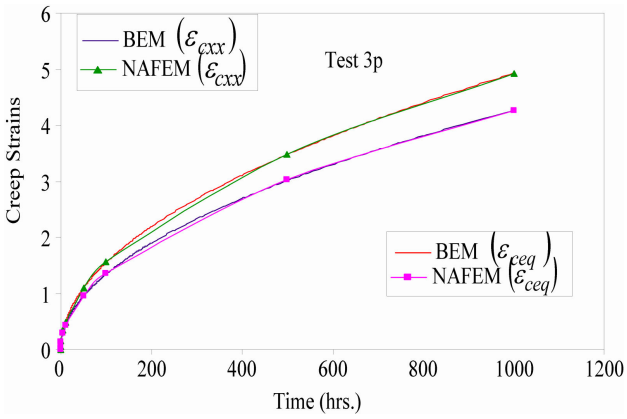

FIGURE 4. Creep strains distribution for a biaxial negative load in a primary creep analysis.

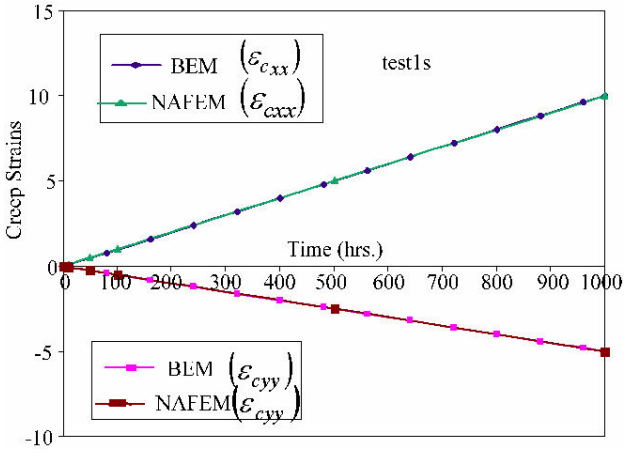

FIGURE 5. Creep strains distribution in the x-directon and the y-direction for secondary creep analysis.

The results of the equivalent creep strain distribution and creep strain in the x-direction are shown in Fig. 4. These results show the parabolic behaviour of the primary creep analysis, which is to be expected for this stage of creep. These results are in very good agreement with NAFEMS' results.

3.5. Test 1s: (uniaxial load)

Similar to the primary creep tests, this example is a square plate subjected to uniaxial stress. This test is a secondary creep and plane stress problem. The geometry, mesh, boundary conditions and material properties are the same as those used in test 1p, except that the creep parameter m=1.0, which defines a secondary creep analysis.

Figure 5 shows the results for creep strain in the x-direction and the y-direction. The computed value of $\dot{\varepsilon}^c_{xx}$ after the final time step is 10.0. These results show straight line behaviour in the secondary creep stage, which is the expected behaviour for this stage of creep. The results are in very good agreement with NAFEMS results.

3.6. Test 2s: (biaxial load)

Similar to the primary creep tests, this example is a square plate subjected to biaxial tensile stress. This test is a secondary creep and plane stress problem. The geometry, boundary conditions, mesh, material properties and creep parameters are the same as those used in test 2p, except that the creep parameter m=1.0 which defines a secondary creep analysis.

Figure 6 shows the results for creep strain in the x-direction and the y-direction. The computed value of $\dot{\varepsilon}^c_{xx}$ after the final time step is 10.0, and the results are the same for the creep strains in the y-direction. These results show straight line behaviour in the secondary creep stage, which is the expected behaviour for this stage of creep. The results are in very good agreement with NAFEMS results.

3.7. Test 3s: (biaxial negative load)

For this example, a square plate subjected to biaxial stress, tension and compression is used. This test is the secondary creep and plane stress problem. The geometry, boundary conditions, mesh, material properties and creep parameters are the same as those used in test 3p, except that the creep parameter m=1.0, which defines a secondary creep analysis.

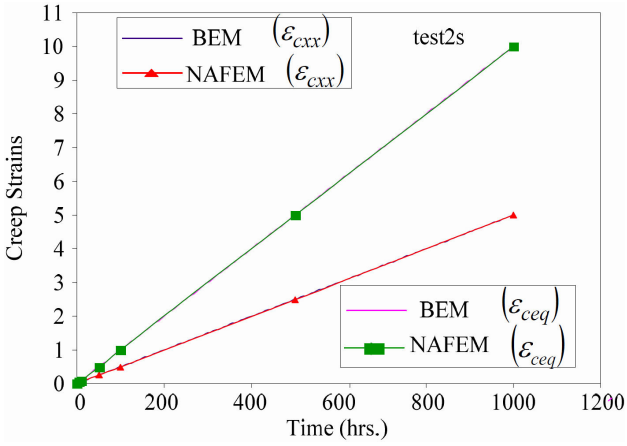

FIGURE 6. Creep strain distribution for a biaxial load in secondary creep analysis.

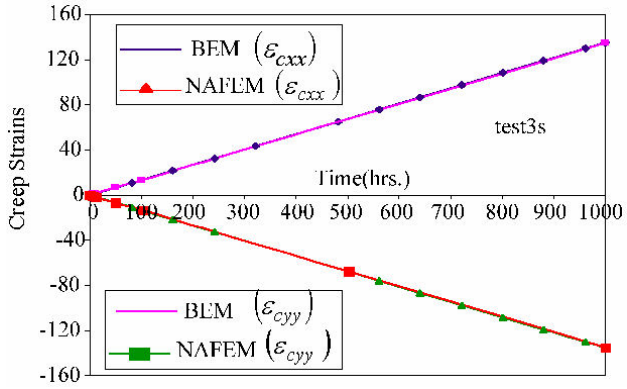

FIGURE 7. Creep strain distribution for a biaxial negative load in secondary creep analysis.

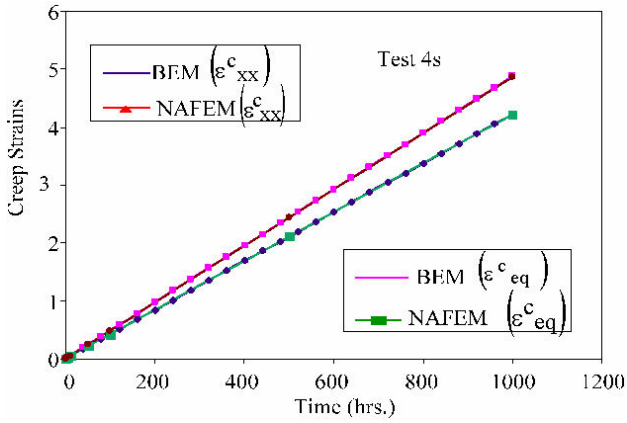

FIGURE 8. Creep strain distribution in a biaxial load.

Figure 7 shows the results for creep strain in the x-and y-directions. The computed value of $\dot{\varepsilon}^c_{xx}$ after the final time step is 120.0 and the creep strains $\dot{\varepsilon}^c_{yy}$ is -120.0. These values are due to the applied load, which in the x-direction is tension and in the y-direction is compression. These results show straight line behaviour in the secondary creep stage, which is the expected behaviour for this stage of creep. The results are in very good agreement with NAFEMS results.

3.8. Test 4s: (biaxial double load)

These tests concern different biaxial tension stresses. The geometry, mesh and boundary conditions are presented in Fig. 1. This test is secondary creep and plane stress problem. The mesh consists of 8 boundary elements and 4 internal cells, as shown in Fig. 1. The material properties and creep parameters are the same as those used in test 3s.

Figure 8 shows the results for creep strain in the x-direction and the equivalent strain. The computed value of $\dot{\varepsilon}^c_{xx}$ after the final time step is 5.0. These results show straight line behaviour in the secondary creep stage, which is the expected behaviour for this stage of creep. The results are in very good agreement with NAFEMS results.

4. Conclusions

The application of the BEM formulation for creep to some benchmark problems was analyzed; good agreement with NAFEMS results was observed for all cases. Also found was a parabolic behaviour in all cases of primary creep; but for secondary creep, there was straight line behaviour in all cases. It is important to notice that in practice the secondary creep analysis is the most used case, but primary creep could be important in some cases.

The BE program was tested for the problems of a square plate. The tests include primary creep in some cases and secondary creep in most cases, and also plane stress and plane strain analysis. The time hardening creep law was applied for all cases of creep. The BEM results are compared with the corresponding finite element solutions obtained, using references where available. The results were found to be in good agreement with the references.

In order to obtain accurate results, it is very important to choose the size of the initial time step. If it is too large, the results will not be accurate. If it is too small, the results will be more accurate but the computational cost and consuming time will be very high. The prescribed tolerances play a very important role and they give the same effect as the initial time step. Since an automatic time step control is used in this work, the maximum and minimum tolerances must be prescribed. In all problems, the minimum tolerance is determined by dividing the maximum tolerance by 10. Therefore, the minimum tolerance is one order less than the maximum tolerance. The solutions improve as the maximum tolerance gets smaller. Because of this, the initial time step and prescribed tolerances must be chosen carefully

Acknowledgements

The authors wish to thank Dr. Alejandro Rodriguez Castellanos for his valuable cooperation in this paper.

1. M.H. Aliabadi, *The Boundary Element Method. Applications in Solids and Structures* (Vol. 2. John Wiley & Sons, Ltd, West Sussex, England 2002).

2. O.C. Zienkiewicz, *The Finite Element Method, McGraw-Hill* (New York, 1971).

3. J.T. Oden, *Finite Elements of Nonlinear Continua* (McGraw-Hill, New York, 1972).

4. I. Fredholm, *Acta Mathematica* **27-390** (1903) 365.

5. S.G. Mikhlin, *Integral Equation* (Pergamon Press, London, 1957).

6. V.D. Kupradze, *Potential Methods in the Theory of Elasticity* (Israel Programms for Scientific Translations, Jerusalem, 1965).
7. T.A. Cruse, *International Journal of Solids and Structures* **5** (1969) 1259.
8. M.A. Jaswon, *Proceedings of the Royal Society of London, Series A* **275** (1963) 23.
9. J.L. Hess and A.M.O. Smith, *Calculation of Potential Flows About Arbitrary Bodies, Progress in Aeronautical Sciences, 8* (Pergamon Press, London 1967).
10. C.E. Massonet, *In Stress Analysis* (Chapter 10, Wiley, London (1965) 198.
11. F.J. Rizzo, *Quarter Journal of Applied Mathematics* **25** (1967) 83.
12. T.A. Cruse, Mathematical Foundations of The Boundary Integral Equation Method in Solid Mechanics. Report No. AFOSR-TR-77-1002, Pratt and Whitney Aircraft Group (1977).
13. J.C. Lachat, *A Further Development of the Boundary Integral Techniques for Elastosatics* (PhD thesis, University of Southampton, (1975).
14. J.C. Lachat and J.O. Watson, *International Journal for Numerical Methods in Engineering* **10** (1976) 991.
15. J.L. Swedlow and T.A. Cruse, *International Journal of Solids and Structures* **7** (1971) 1673.
16. P. Riccardella, *An Implementation of the Boundary Integral Technique for plane problems of Elasticity and Elastoplasticity* (PhD Thesis, Carnegie Mellon University, Pitsburg, PA 1973).
17. P.K. Banerjee and G.C.W. Mustoe, *The boundary element method for two-dimensional problems of elasto-plasticity. Recent Advances in Boundary Element Methods*, C.A. Brebbia (ed.), (Pentech Press, Plymouth, Devon, UK, 1978) 283.
18. P.S. Theocaris and E. Marketos, *Journal of Mechanics and Physics of Solids* **12** (1964) 377.
19. J.C.F. Telles, C. Brebbia, *Appl. Math. Modelling* **3** (1979) 466.
20. V.M.A. Leitao, *Topics in Engineering* **21**, (Computational Mechanics Publications, U.K. 1994).
21. A.A. Becker, and T.H. Hyde, *NAFEMS report* (1993) R0027.
22. E. Pineda, *Dual Boundary Element Analysis for Creep Fracture* (PhD thesis, University of London, 2006)